A vision based feedback mechanism for 6-DOF Stewart Platform

UTKU BÜYÜKŞAHİN

A vision based feedback mechanism for 6-DOF Stewart Platform

Utku BÜYÜKŞAHİN

Mechatronics Engineering Department, Yıldız Technical University,
Beşiktaş, İstanbul-TURKEY
e-mail: buyuksah@yildiz.edu.tr

Abstract

Eyes are the most ubiquitous sensors of humankind. However, "Vision Based Sensors" are not as common as what this fact would suggest. A survey of the previous work on image processing would reveal that the bulk of the research in this area have been conducted since the year 2000. These facts clearly show that image processing is the technology of our century, and is very open to further development.

In this work, a system that combines a classical mechanism of the 20th century with the recent technology of the 21st century is presented and the design, theoretical background, the software algorithm for a vision based, low cost feedback mechanism is given. Simulation results based on the image processing of a 3-D animated model of a Stewart Platform through the aforementioned feedback system are also included. These results demonstrate that the software performed all necessary tasks to compute the leg lengths successfully.

Key Words: *Stewart Platform, image recognition, feedback mechanism*

1. Introduction

With the emergence of unmanned flying vehicles, the flight simulators utilizing the Stewart Platform will no longer be just tools for pilot training, but become full-fledged flight units that pilots use to operate these unmanned crafts. Tomorrow's battlefields may look like today's "internet cafe"s, where a large number of flight simulators are found in a large room. However, this can only be made possible with the reduction in the extremely high cost of the existing flight simulators. The feedback mechanism of the Stewart platform constitutes a substantial portion of these high costs, and it is impossible to consider removing the feedback mechanism from the control of such a complicated moving system. We believe the right approach to this problem is to develop lower cost feedback mechanisms instead of designing systems without feedback.

The reliability of a feedback mechanism in a system with many joints depends on the location where movement is measured and the rigidity and the reliability of the actual moving joints. This can be easily understood by considering the example of an automobile that has just braked and skidding. The internal feedback mechanism displays "0" on the speedometer (as the wheels are locked); however anyone looking from the outside can easily tell that the automobile is still moving. The same applies to the movement of a Stewart

Platform. There are many moving joints that connect the upper platform to the lower, and these joints all have a certain amount of gap in them. When these are all considered, it should be clear that a feedback mechanism that observes the platform from outside through cameras is very advantageous.

Since its introduction in 1965 [1], Stewart Platform has been constantly studied and improved. The history of the Stewart Platform and the benefits of using these in flight simulators to enable pilot training without risking to one's life are presented in [2]. The calculations including direct and inverse kinematics of Stewart Platform with 6 degrees of freedom are studied in [3], [4], [5], [6],and [7]. Designing a CNC milling machine using a Stewart Platform with 6 degrees of freedom is presented in [8]. Using a 3×3 Stewart Platform as the control stick for a flight craft, and providing the kinematic and dynamic equations of the system using the Bond Graph method are presented in [9].

Although eyes are the most ubiquitous sensors of the human, "Vision Based Sensors" are still not at a level where they deserve to be. Bulk of the work done to study image processing has happened since 2000s, suggesting that this is an area ripe for technological advancement, and probably, the technology of our century.

There is a constant influx of studies on signal processing in academic literature. A system that will identify license plates using the existing observation cameras is introduced in [10]. An approach for image recognition based on a hybrid methods that combines 2 types of fuzzy logic modular neural networks and the Sugena integral are introduced in [11]. Identifying the color edge is one of the most critical steps in color image processing is stated in [12]. 1-D and 2-D algorithms that identify a 400x300 pixel "Stop" sign in less than 25 milliseconds are presented in [13]. An image processing and Bayes network that observes the movements of a student getting distant learning is introduced in [14]. An image processing application called "chicken wing" to determine the sex of chicks has been developed in [15]. In the next section we will introduce the general structure of our system, the software development for the feedback mechanism and the equations used. This 3rd section will introduce the simulations conducted, and 4th section will conclude the article.
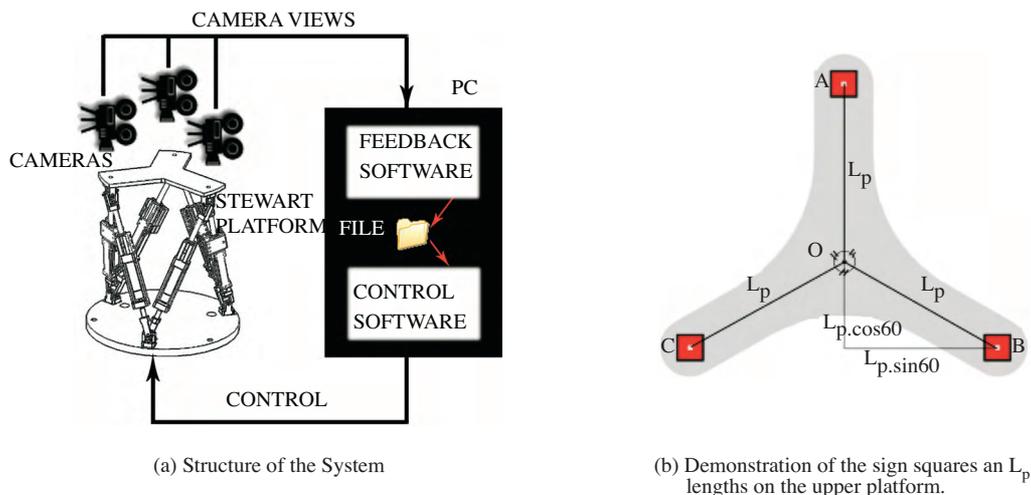
2. System

(a) Structure of the System

(b) Demonstration of the sign squares an L_p lengths on the upper platform.

Figure 1. System.

2.1. Structure of the system

As seen in Figure 1a, the system consists of one 3×3 Stewart Platform with 6 degrees of freedom, square signs that are placed on the top plane at the centers of joints (seen more clearly in Figure 1b), 3 cameras that are placed on the normals of this joints and focused at the centers of the squares and a Personal Computer (PC).The PC runs two software programs: one that was developed specifically for this project to process the images obtained from these cameras, and another one that handles the controls of the Stewart Platform [9]. The reasoning behind using 3 cameras in the systems as opposed to one is to avoid the perspective problems inherent in a single camera system and to increase the resolution of the system. As all three cameras are placed on the normals of the centers of the sign squares, any displacement in the Z axis only affects the dimensions of the squares but does not impact the corner coordinates of the computation triangle. Resolution is increased by more than 3x as the center of the platform (useless for calculations) is not included in the captured images.

As the cameras capture 2-D images, calculating the displacements in X and Y coordinates (ΔX and ΔY) are relatively trivial. The main problem is to be able to sense movements in the 3rd dimension (Z coordinate). There are various methods that can be used to achieve this, however using a combination of these methods increase the likelihood of getting reliable results.

The cameras in the current system are placed outside the Stewart Platform, looking down on it. The system can also be constructed by enclosing the cameras in the platform, looking up on the sign squares.

Everything else being equal, moving the sign squares (and of course the cameras focused on the centers of these squares as well) outward on a straight line (e.g., point A along the OA line) - in other words, increasing Lp - would allow the detection of movement other than ΔX and ΔY with higher resolution. With the same reasoning, moving the sign squares towards the center hurts the measurement resolution.

2.2. Software
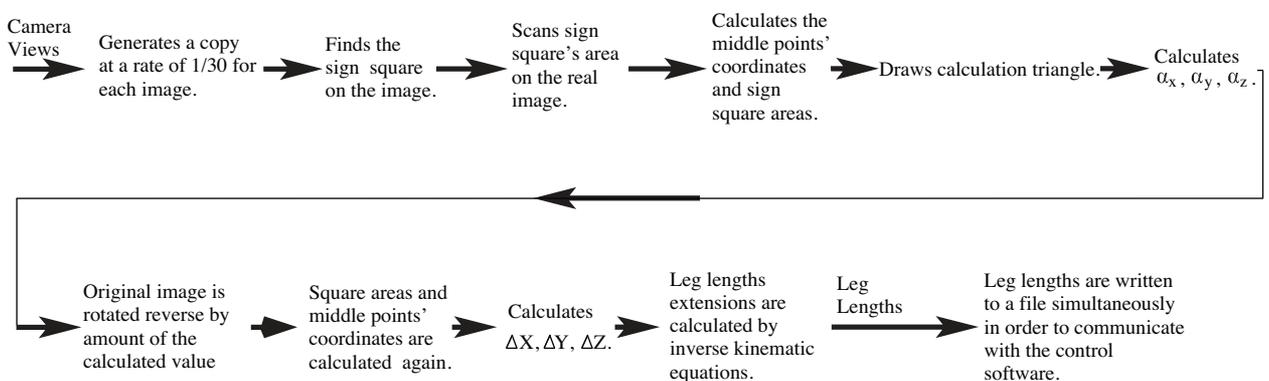
Figure 2. Common flow diagram of the Software.

The software for this application has been developed using Visual Basic 6 (VB6) programming language. To work around the possible performance related problems of VB6 in image processing, the processing on the images collected are done before the images are loaded to the memory, hence making the image processing steps independent of the language used.

The most computationally intensive portion of the image processing step is the scanning of the entire image to detect the location of the sign squares. The complexity of this process increases with the resolution

of the camera; therefore the images collected from cameras can be scaled down 30-100X before processing. In our current algorithm, the images are scaled down 30X to achieve a $30^2 = 900$X performance enhancement. The critical point in this process is to avoid choosing a scale factor so high that the sign squares become too small to detect. Once the location of the sign square is detected, the immediate area of the square is re-scanned in its actual resolution to obtain precise coordinate and area measurements.
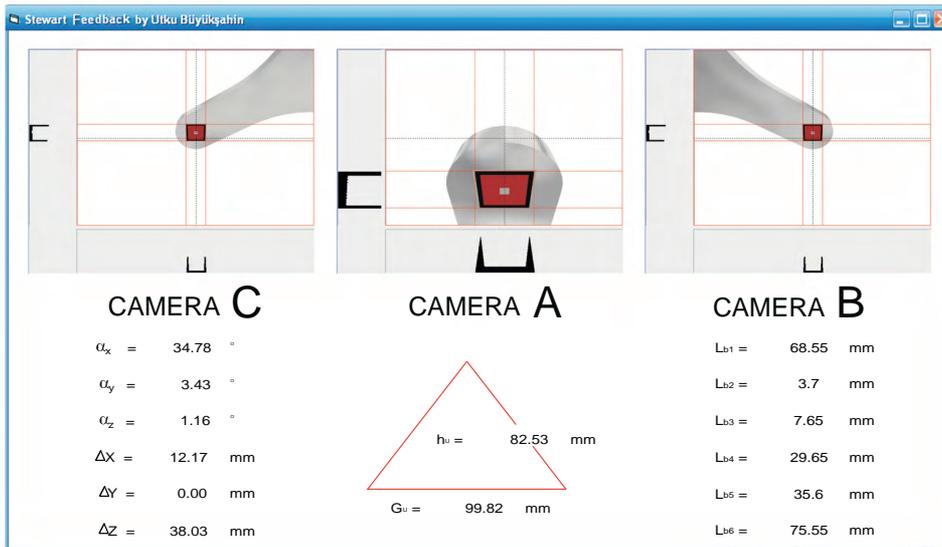

Figure 3. Screenshot of the software while running.

As the process of scanning the image in a loop is a relatively expensive operation, it has not been combined with the control software of the Stewart Platform, thus enabling concurrent operation of these two pieces of software and better sharing of the computing resources (e.g., letting the OS schedule the two software programs to run on different cores on a multi-core PC). The feedback software provides the leg lengths to the control software in real-time by writing the values continuously to a file that is then read by the control software. The control software uses these values as feedback to solve the kinematic equations.

2.3. Calculations

2.3.1. Calculations of bending and translational values

The software that searches and finds the middle point' special color from the images coming from three cameras, divides the points' coordinate which is in the form of pixels to a gain value that is calculated by pixel quantity that corresponds to 1 mm. Thus, the obtained values are in millimeters unit. As seen in figure 4, addition of the "0" points of all cameras to A, B, C points give the coordinate of $X_A, Y_A, X_B, Y_B, X_C, Y_C$. After that, the software compares the areas of the squares in order to determine the relative level of the points A, B, C by using the perspective property which says higher is larger in area. (e.g. A: Highest B: Lowest C: Middle) The coordinates that are calculated from the camera views are used to build up the "Calculation Triangle" which will be used in following calculations.

With the equation (1), G_u, which is the width of the calculation triangle, is calculated

$$G_u{}^{\shortmid} = |A{}^{\shortmid}B{}^{\shortmid}| = [(XB{}^{\shortmid} - XC{}^{\shortmid})^2 + (YB{}^{\shortmid} - YC{}^{\shortmid})^2]^{1/2} \qquad (1)$$
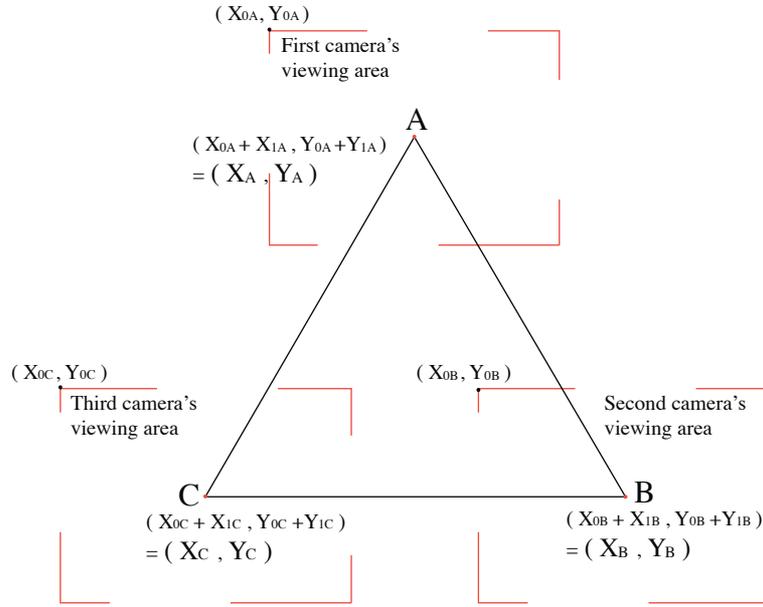
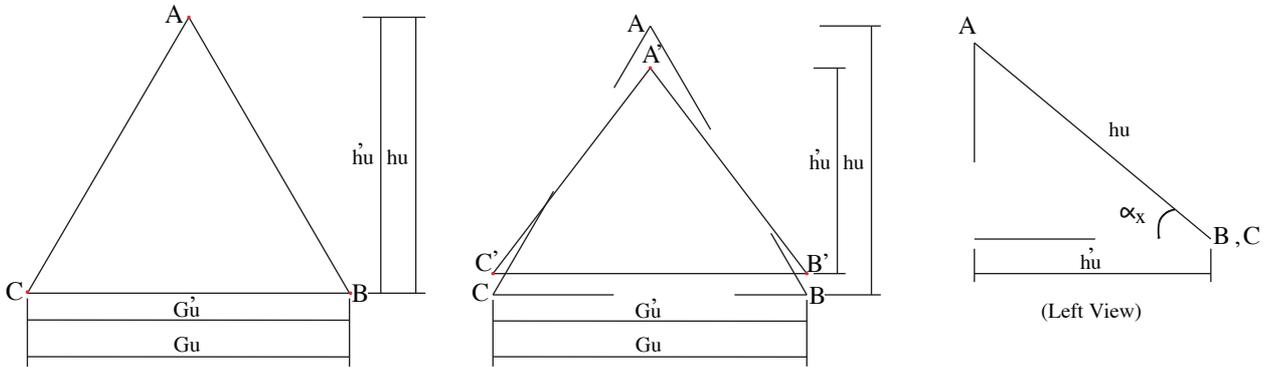**Figure 4**. All three camera's viewing area and A, B, C points' coordinates.

Figure 5. Calculations.

With the equation (2), h_u, which is the height of the calculation triangle, is calculated

$$h_u = |A'B'|.\sin[\arctan[(Y_{A'} - Y_{B'})/(X_{A'} - X_{B'})] - \arctan[(Y_{B'} - Y_{C'})/(X_{B'} - X_{C'})]] \tag{2}$$

With the equation (3), a_y, which is the rotating angle at the Y axis, is calculated.

$$a_y = \arccos(Gu'/Gu) \tag{3}$$

With the equation (4), a_x, which is the rotating angle at the X axis, is calculated.

$$a_x = \arccos(hu'/hu) \tag{4}$$

With the equation (5), a_z, which is the rotating angle at the Z axis, is calculated from the slope of the line $|B'C'|$.

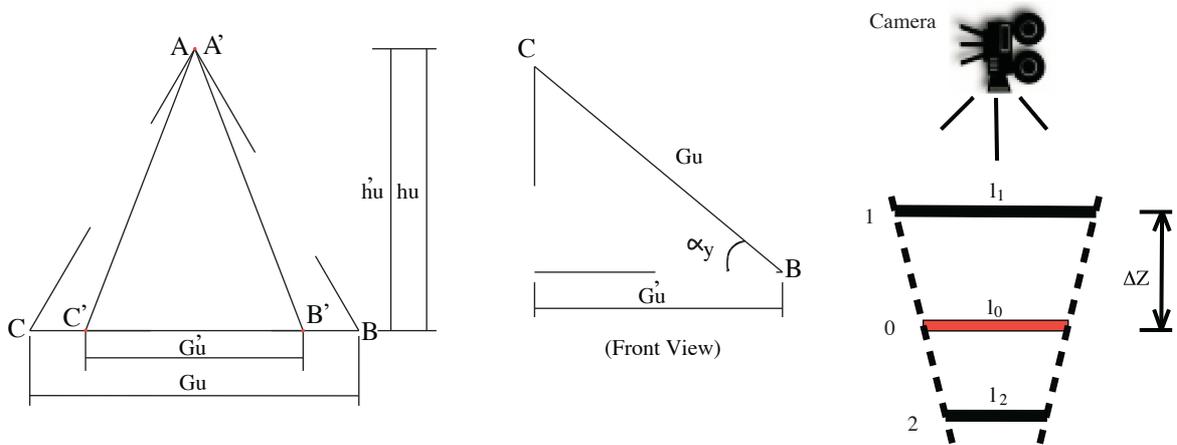$$a_z = \arctan[(YB' - YC')/(XB' - XC')] \tag{5}$$

Figure 6. Calculations.

After a_x, a_y, a_z angles are calculated, the software rotates the image in the opposite direction ($-a_x$, $-a_y$, $-a_z$) to obtain the straightened image. On the straightened image, only translations (ΔX, ΔY, ΔZ) are present.

$$X_A - X_{A'} \neq 0 \tag{6}$$

$$Y_A - Y_{A'} \neq 0 \tag{7}$$

In case of confirmation of the equation (6), X is shifted by the amount of calculation's result. And in case of confirmation of the equation (7), then Y is shifted by the amount of calculation's result. ΔZ translation's amount is calculated by using the similarity and the ratio of sign squares' areas to the "0" position which is calculated by straightened view of sign square's areas.

$$\Delta Z = (l_1 - l_0).\Delta_{ascending} \tag{8}$$

The rising gain ($\Delta_{ascending}$) in equation number (8) is obtained empirically for different rising values. As a result of all these calculations a_x, a_y, a_z, ΔX, ΔY, ΔZ values are being calculated. In the following sections by using all bending and translational values of upper platform, "Inverse Kinematics" will be applied to calculate each leg length.

2.3.2. Inverse kinematic equations

In this section inverse kinematic calculations for a 3×3 Stewart Platform is given.

The software provides simultaneously X and Y coordinates of the A, B, C points. In order to find the leg lengths, Z coordinates of A, B, C points are needed to be calculated by using obtained bending and translational values. Z coordinate of point A can be obtained from equation (8). Z coordinates of points B and C can be obtained from equation (9).

$$Z_A = \pm Lp.\sin a_x.\sin(90 - a_y) + \Delta Z \tag{9}$$

$$Z_{B,C} = Lp.\sin 60.\sin a_y \pm Lp.\sin a_x.\sin(90 - a_y).\cos 60 + \Delta Z \tag{10}$$

In the equation (9) and (10), ΔZ is the translation that is done at Z axis. In order to calculate the leg lengths, Z coordinates of the lower platform must be given relatively to a Z reference point. "$\pm$" signs that

take place in the equation (9) and (10), represents the situations of descending and ascending. As the lower platform and the joint coordinates are fixed, the coordinates are constant. These values are: $[X_1a \ , \ Y_1a \ , \ Z_1a]$ Ö ; $[X_6a \ , \ Y_6a \ , \ Z_6a \ ]$. In the following equations (11) to (16), coordinates of the points A, B, C and the lower joints are used to calculate the leg lengths.

$$L_1 = [(X_A - X_{1a})^2 + (Y_A - Y_{1a})^2 + (Z_A - Z_{1a})^2]^{1/2} \tag{11}$$

$$L_2 = [(X_A - X_{2a})^2 + (Y_A - Y_{2a})^2 + (Z_A - Z_{2a})^2]^{1/2} \tag{12}$$

$$L_3 = [(X_B - X_{3a})^2 + (Y_B - Y_{3a})^2 + (Z_B - Z_{3a})^2]^{1/2} \tag{13}$$

$$L_4 = [(X_B - X_{4a})^2 + (Y_B - Y_{4a})^2 + (Z_B - Z_{4a})^2]^{1/2} \tag{14}$$

$$L_5 = [(X_C - X_{5a})^2 + (Y_C - Y_{5a})^2 + (Z_C - Z_{5a})^2]^{1/2} \tag{15}$$

$$L_6 = [(X_C - X_{6a})^2 + (Y_C - Y_{6a})^2 + (Z_C - Z_{6a})^2]^{1/2} \tag{16}$$

L_1, L_2, L_3, L_4, L_5, L_6 values are the distances between the joint points of upper and bottom platform which are calculated from equations (11) through (16). In order to find leg extension lengths, upper joint's height, bottom joint's height and motor's height at the minimum position must be subtracted from these values.

$$L_{b1} = L_1 - L_{1higherjoint} - L_{1lowerjoint} - L_{1motorlength} \tag{17}$$

$$L_{b2} = L_2 - L_{2higherjoint} - L_{2lowerjoint} - L_{2motorlength} \tag{18}$$

$$L_{b3} = L_3 - L_{3higherjoint} - L_{3lowerjoint} - L_{3motorlength} \tag{19}$$

$$L_{b4} = L_4 - L_{4higherjoint} - L_{4lowerjoint} - L_{4motorlength} \tag{20}$$

$$L_{Lb5} = L_5 - L_{5higherjoint} - L_{5lowerjoint} - L_{5motorlength} \tag{21}$$

$$L_{b6} = L_6 - L_{6higherjoint} - L_{6lowerjoint} - L_{6motorlength} \tag{22}$$

L_1, L_2, L_3, L_4, L_5, L_6 values that are obtained from equations (17) through (22), are the output values that is given by the software as the feedback values of the platform.

3. Simulations

To test the system, a Stewart Platform is drawn through a 3-D design software and the sign squares were placed in the correct locations. 3 cameras are defined in the software and placed in the locations they would be in the real system (looking down on the system along the normal through the center of each square). The system is then set to perform various tilts and displacements, and the images captured through the cameras have been fed to the feedback software as camera images. The software has then computed the leg lengths with perfect accuracy.

4. Results

In this work, we have introduced a novel image processing based feedback mechanism for a Stewart Platform. We derived the equations required for the system, and introduced the steps the necessary software algorithm takes to achieve the intended results. We have also simulated a 3-D model of the Stewart Platform formed in a drawing software, obtained images that contain the movement of the platform, and fed these images to the feedback software. The feedback software has then successfully calculated the leg lengths. Our simulations and animations demonstrate that the resolution of the system is < 0.1mm for displacements and < 0.1 degrees for tilts. These values are well within the expected error margins.

This work shows that it would be possible to get very satisfactory and low cost results from a feedback system built with components easily obtained from a computer hardware store, printouts of sign squares and special software designed for this purpose. This eliminates the need for the very high cost hardware feedback systems. The cost advantage and relative simplicity of the system suggest that we may see these systems used frequently in the future.

The performance of the system is open to improvements with the increases in camera resolutions and PC computing power. The plans to implement this system on a real Stewart Platform as the next step are in place and the work to achieve this is already under way.

References

[1] D. Stewart, "A Platform with Six Degrees of Freedom", Proc. Instn. Mech. Engrs., vol.80, pp.371-386, 1965.

[2] E. Anli, H. Alp, S.N. Yurt, I. Ozkol. "Paralel mekanizmalarin kinematigi, dinamigi ve calisma uzayi." Havacilik ve uzay teknolojileri dergisi. Volume 2 Issue 1 (19-36), January 2005.

[3] C.C. Nguyen, Z.L. Zhou, S.S. Antrazi, C.E. Campbell Jr. "Efficient Computation of Forward Kinematics and Jacobian Matrix of a Stewart Platform-based Manipulators." Southeastcon, IEEE Proceedings of, 7-10 Apr 1991.

[4] P. Nanua, K.J. Waldron, V. Murthy. "Direct Kinematic Solution of a Stewart Platform." Robotics and Automation, IEEE Transactions on,1990.

[5] B. Dasgupta, T. S. Mruthyunjaya. "A Newton-Euler Formulation for the Inverse Dynamics of the Stewart Platform Manipulator." Mech. Mach. Theory Vol. 33, No. 8, pp. 11351152, 1998.

[6] S.H. Lee, J.B. Song, W.C. Choi, D. Hong. "Position Control of a Stewart Platform Using Inverse Dynamics Control with Approximate Dynamics." Mechatronics 13 605-619, 2003.

[7] I. Davliakos, E. Papadopoulos. "A Model-Based Impedance Control of a 6-Dof Electrohydraulic Stewart Platform." European Control Conference 2007, Kos, Greece, July 2-5, 2007.

[8] Y. Ting, Y.S. Chen, H.C. Jar. "Modeling and Control for a Gough-Stewart Platform CNC Machine." Journal of Robotic Systems 21(11), 609-623, 2004.

[9] V.E. Omurlu, U. Buyuksahin, I. Yildiz, A. Unsal, A. Sagirli, S.N. Engin, I.B. Kuukdemiral , "A Stewart Platform as a FBW Flight Control Unit for Space Vehicles." Recent Advances in Space Technologies - RAST 2009, Istanbul, Turkiye, 11-13 June, 2009.

[10] Y.P. Huang. "A Back Propagation Based Real-Time License Plate Recognition System." International Journal of Pattern Recognition and Artificial Intelligence Vol. 22, No. 2 233-251, 2008.

[11] O. Mendoza, P. Melin, G. Licea. "A Hybrid Approach for Image Recognition Combining Type-2 Fuzzy Logic, Modular Neural Networks and the Sugeno Integral." Information Sciences 179 2078-2101, 2009.

[12] G. Li, L. Min, H. Zang. "Color Edge Detections Based on Cellular Neural Network. International Journal of Bifurcation and Chaos", Vol. 18, No. 4 1231-1242, 2008.

[13] J. Wu, Y. (J.) Tsai. "Enhanced Roadway Inventory Using a 2-D Sign Video Image Recognition Algorithm." Computer-Aided Civil and Infrastructure Engineering 21 369-382, 2006.

[14] K.A. Hwang, C.H. Yang. "Learner Attending Auto-Monitor in Distance Learning Using Image Recognition and Bayesian Networks." Expert Systems with Applications 36, 11461-11469, 2009.

[15] Y. Tao, Z. Chen, C.L. Griffis. "Chick Feather Pattern Recognition." IEE Proc.-Vis. Image Signal Process., Vol. 151, No. 5, October 2004.